ELSEVIER

Journal of Alloys and Compounds 248 (1997) 70–76

Journal of ALLOYS AND COMPOUNDS

# Thermoelectric and magnetic properties of $Cr_{1-x}V_xSi_2$ solid solutions

H. Hohl*, A.P. Ramirez, T.T.M. Palstra, E. Bucher

*Lucent Technologies, Bell Laboratories, PO Box 636, Murray Hill, NJ 07974, USA*

Received 26 July 1996; revised 14 August 1996

**Abstract**

$Cr_{1-x}V_xSi_2$ solid solutions have been prepared in the range $0 \le x \le 1$. The thermopowers, resistivities, and magnetic susceptibilities of the solid solutions vary smoothly with composition and reveal a continuous transition from degenerate semiconducting ($x = 0$) to metallic ($x = 1$) behavior. $S^2/\rho$ ratios of the solid solutions are less than those of pure $CrSi_2$. The thermoelectric properties of the solid solutions can be described in terms of a free-electron model, whereas an effective mass of 15 $m_e$ has to be assumed in order to explain the results of magnetic measurements.

*Keywords:* Refractory disilicides; Vegard's law; Thermopower; Resistivity; Magnetic susceptibility

## 1. Introduction

As a semiconductor, $CrSi_2$ is unique among the otherwise metallic refractory metal disilicides $RSi_2$ formed by the Group IVB–VIB elements. An indirect bandgap of 0.35 eV, which corresponds well with the 3–5 μm band of atmospheric transparency, makes this compound a potential candidate for infrared detector applications [1]. $CrSi_2$ has also found interest as a thermoelectric conversion material because of its high-temperature stability and promising thermopower. The thermoelectric figure of merit

$$Z = \frac{S^2}{\rho\kappa} \quad (1)$$

which can be calculated from the thermopower $S$, the resistivity $\rho$ and the thermal conductivity $\kappa$, was found to be $2.8 \times 10^{-4}\ K^{-1}$ at room temperature [2,3]. This is about one order of magnitude smaller than values achieved on $Bi_2Te_3$ alloys ($Z \approx 3 \times 10^{-3}\ K^{-1}$), the best thermoelectric materials known at present [4].

When alloying $CrSi_2$ with one of the other refractory disilicides, a continuous transition from semiconducting to metallic behavior is to be expected if a complete solid solution is formed. This would allow the adjustment of material parameters according to specific needs, e.g. in order to extend the photoresponse of the material to longer wave lengths or to hopefully find a composition with a higher thermoelectric figure of merit. A necessary prerequisite for solid solution formation is that both constituents of the alloy are isostructural. The refractory disilicides crystallize with a variety of closely related low-symmetry structures, namely orthorhombic C54 (R = Ti), orthorhombic C49 (R = Zr, Hf), hexagonal C40 (R = V, Nb, Ta, Cr), and tetragonal $C11_b$ (R = Mo, W) [5]. The only likely candidates for pseudo-binary solid solution formation with $CrSi_2$ are therefore $VSi_2$, $NbSi_2$, and $TaSi_2$.

Recently, thin films of $Cr_{1-x}V_xSi_2$ have been grown on (100) silicon wafer substrates; the dependence of the infrared reflectance, infrared transmittance and room temperature resistivity on composition has been reported [6]. In order to further investigate this system we prepared bulk $Cr_{1-x}V_xSi_2$ samples and performed temperature dependent measurements of the thermopower, resistivity and magnetic susceptibility.

## 2. Experimental

Samples of composition $Cr_{1-x}V_xSi_2$ ($x = 0$, 0.10, 0.20, 0.30, 0.39, 0.49, 0.74, 1) were prepared by melting together chromium (MRC, Van Arkel granules, 4N8), vanadium (Atomergic Chemetals, dendritic crystals, 3N+) and silicon (JMC, lump, 5N5) in an arc furnace. This synthesis method was chosen because the end members of the series are known to melt congruently at high temperatures: 1490 °C ($CrSi_2$) and 1677 °C ($VSi_2$) [7]. The argon atmosphere in the furnace was gettered by melting a piece of zirconium prior to the actual samples.

*Corresponding author.


PII S0925-8388(96)02646-1

Both chromium and vanadium were etched in hot dilute hydrochloric acid and premelted in the arc furnace in order to remove oxides and volatile impurities. Since chromium exhibits a significant vapor pressure at elevated temperatures, care had to be taken to keep the chromium loss at a minimum. This problem was overcome by placing silicon on top of the chromium and vanadium spheres, thereby pouring a hot melt of silicon on the metals in order to react the three elements. A slight excess of chromium (0.1%) was added to compensate for unavoidable loss. Every sample was turned over and remelted two times to ensure homogeneity. The resulting buttons, each of about 1.5 g in mass, were then wrapped in tantalum foil and annealed to 1000 °C for a week in evacuated and sealed quartz tubes. Bars with dimensions $0.7\times1.2\times8\ mm^3$ were cut from the buttons with a diamond blade wheel saw.

The samples were characterized through powder diffraction patterns collected on a Philips PW-1710 powder diffractometer. $LaB_6$ was used as standard. The lattice parameters were obtained by a least-squares refinement technique. Up to 20 diffraction peak positions in the range $2\theta = 20–90°$ were evaluated for each refinement. An MMR SB-100 Seebeck controller was used to measure the thermopower of the samples in an experimental set-up which employs copper–sample–copper and copper–constantan–copper differential thermocouples. The resistivity was measured with a Linear Research LR-700 resistance bridge, a linear four-probe set-up with alternating current. Silver epoxy was used for sample contacts in the thermopower and resistivity measurements. The magnetic susceptibility of the samples was measured with a Quantum Design SQUID magnetometer.

## 3. Results

Sample weights were checked after the first melting process and matched the stoichiometric values typically within 0.01% (assuming all loss to be chromium). When the samples were further remelted small amounts of material were found to splinter off. This behavior was most pronounced on the $x = 0.74$ sample, which repeatedly broke into pieces when congealing from the melt. The loss of already reacted and therefore nearly stoichiometric material during remelting is not considered to have affected the overall compositions of the samples significantly.

Powder diffraction patterns of the samples were indexed assuming hexagonal unit cells. The dependence of the lattice parameters $a$ and $c$ on the sample composition is shown in Fig. 1. Values found for the end members $CrSi_2$ ($a = 442.83(2)$, $c = 636.92(5)$ pm) and $VSi_2$ ($a = 457.22(4)$, $c = 637.37(8)$ pm) are in good agreement with literature data [8]. The molar volumes of the solid solutions, calculated from the unit cell volumes $v = (\sqrt{3}/2)a^2c$ by

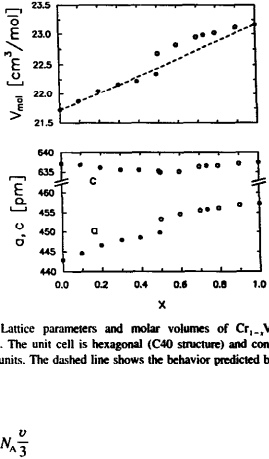


Fig. 1. Lattice parameters and molar volumes of $Cr_{1-x}V_xSi_2$ solid solutions. The unit cell is hexagonal (C40 structure) and contains three formula units. The dashed line shows the behavior predicted by Vegard's law.

$$V_{mol} = N_A\frac{v}{3} \qquad (2)$$

are shown in the upper portion of Fig. 1. According to Vegard's law, unit cell volumes (and molar volumes) are expected to vary linearly with composition if solid solutions are formed by random substitution of atoms. (Vegard's law is generally referred to as a linear dependence of lattice parameters on composition [9,10]. However, a linear variation of the unit cell volume implies a linear variation of the lattice parameters only in compounds with cubic symmetry, where $\Delta a/a_0 \approx (1/3)\Delta v/v_0$. The dependence of lattice parameters on composition in solid solutions with lower symmetry cannot be predicted even if Vegard's law was found to be obeyed [11].) This law is well obeyed for $x \le 0.49$, whereas the sample with $x = 0.74$ shows a higher molar volume than predicted. Additionally prepared samples (not annealed after arc melting and not used for any further measurements), shown as open circles in Fig. 1, confirm this positive deviation from Vegard's law in the range $x \ge 0.5$. The abrupt change in $V_{mol}$ near $x = 0.5$ is caused by an abrupt change of the unit cell parameter $a$ solely, whereas $c$ varies smoothly over the entire range $0 \le x \le 1$.

Resistivity measurements of the $Cr_{1-x}V_xSi_2$ solid solutions are shown in Fig. 2. Stoichiometric $CrSi_2$ is known to be a degenerate semiconductor having a hole concentration of several $10^{20}\ cm^{-3}$ at room temperature; excess chromium atoms are supposed to act as acceptors in the compound [12–14]. This explains why the resistivity curve of $CrSi_2$ in Fig. 2 shows a slight increase with temperature rather than a semiconductor-like behavior, $d\rho/dT < 0$. A room temperature resistivity of $5.4\times10^{-3}\ \Omega$ cm is found

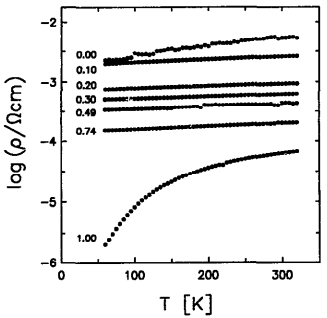


Fig. 2. Temperature dependence of the resistivity for $Cr_{1-x}V_xSi_2$ solid solutions in a semi-logarithmic plot.

for stoichiometric $CrSi_2$. Substitution of chromium by vanadium gradually lowers the resistivities of the solid solutions; the temperature dependence of the resistivity, however, does not change significantly for vanadium contents of up to $x = 0.74$. $VSi_2$, the end member of the series, shows a metallic resistivity behavior $\rho(T) = \rho_0 + \alpha T$ and $\alpha = 2.9 \times 10^{-7}\ \Omega\,cm\,K^{-1}$. The room temperature resistivity of $VSi_2$ is $6.3 \times 10^{-5}\ \Omega\,cm$.

All of the samples show positive absolute thermopowers with an approximately linear temperature dependence (Fig. 3). The room temperature thermopowers $S$(300 K) of the $Cr_{1-x}V_xSi_2$ solid solutions are greatly affected when chromium is substituted by vanadium. Starting at 73.5 $\mu V\,K^{-1}$ ($x = 0$), the thermopower drops to 26.6 $\mu V\,K^{-1}$ when a vanadium content of $x = 0.1$ is added. Further addition of vanadium reduces the thermopower gradually until a value of 6.3 $\mu V\,K^{-1}$ is reached for $x = 1$.

Since the thermal conductivities $\kappa$ of the solid solutions are not expected to be subject to dramatic changes, the dependence of the thermoelectric figure of merit (Eq. (1)) on composition will be discussed in terms of the ratio $S^2/\rho$ only. A room temperature value of $S^2/\rho = 1\ \mu W\,K^{-2}\,cm^{-1}$ is found for stoichiometric $CrSi_2$. When substituting chromium by vanadium in $Cr_{1-x}V_xSi_2$, both the thermopower and the resistivity of the samples are lowered. The overall effect is a reduction of $S^2/\rho$ to values between 0.2 and 0.6 $\mu W\,K^{-2}\,cm^{-1}$, i.e. it is not possible to increase the thermoelectric figure of merit of $CrSi_2$ by alloying it with $VSi_2$. The resistivity of $CrSi_2$, however, can be lowered without affecting the thermopower by adding a slight excess (approximately 1%) of chromium. A room temperature value of 5 $\mu W\,K^{-2}\,cm^{-1}$ was achieved in this way. This is still one order of magnitude smaller than values achieved by $Bi_2Te_3$ based materials which combine thermopowers around 200 $\mu V\,K^{-1}$ with resistivities of $10^{-3}\ \Omega\,cm$ at room temperature.

Temperature dependent susceptibility measurements of $Cr_{1-x}V_xSi_2$ solid solutions are shown in Fig. 4. The room temperature susceptibility of $CrSi_2$ is $-52 \times 10^{-6}\,cm^3\,mol^{-1}$. Only an insignificant temperature dependence is observed for the magnetic susceptibility of the compound. When chromium is substituted by vanadium in $Cr_{1-x}V_xSi_2$, charge carriers are introduced in the system. These carriers give rise to paramagnetic susceptibility contributions and shift the magnetic susceptibility towards

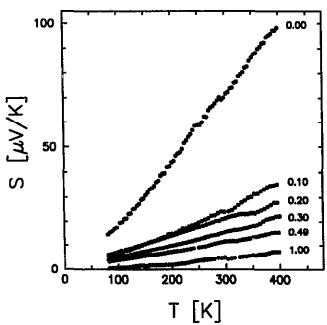


Fig. 3. Temperature dependence of the thermopower for $Cr_{1-x}V_xSi_2$ solid solutions.

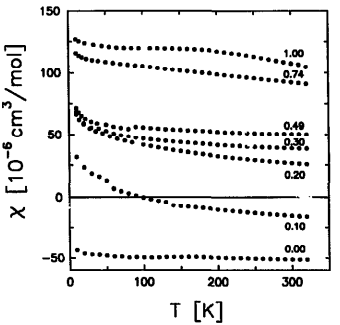


Fig. 4. Temperature dependence of the magnetic susceptibility for $Cr_{1-x}V_xSi_2$ solid solutions. The data are given in units of the electromagnetic cgs-system.

Table 1
Generalized Curie–Weiss fits $\chi = \chi_0 + C/(T-\theta)$ to the magnetic susceptibilities of $Cr_{1-x}V_xSi_2$ solid solutions and corresponding susceptibility contributions of permanent magnetic moments at room temperature $\chi^{CW}(300\,K)$

| $x$ | Fit range (K) | $\chi_0$ ($10^{-6}$ cm$^3$ mol$^{-1}$) | $C$ ($10^{-4}$ K$^{-1}$) | $\theta$ (K) | $\chi^{CW}(300\,K)$ ($10^{-6}$ cm$^3$ mol$^{-1}$) |
|---|---|---|---|---|---|
| 0.00 | 10–110 | −51.2 | 1.85 | −14.5 | 0.6 |
| 1.10 | 10–340 | −27.2 | 43.99 | −65.4 | 12.0 |
| 0.20 | 20–320 | 8.2 | 83.09 | −149.4 | 18.5 |
| 0.30 | 20–320 | 31.7 | 2.64 | −76.8 | 7.0 |
| 0.39 | 10–320 | 33.6 | 7.68 | −24.2 | 2.4 |
| 0.49 | 10–85 | 50.7 | 3.59 | −7.7 | 1.2 |
| 0.74 | 10–50 | 106.2 | 1.41 | 4.8 | 0.5 |
| 1.00 | 10–40 | 119.4 | 1.26 | −7.4 | 0.4 |

more positive values. A magnetic susceptibility of $+107\times10^{-6}$ cm$^3$ mol$^{-1}$ is found for $VSi_2$ at room temperature.

It is evident that some of the susceptibility curves in Fig. 4 also exhibit Curie–Weiss-like temperature dependences, which indicate the presence of permanent magnetic moments. We therefore analysed the magnetic susceptibilities in terms of a generalized Curie–Weiss law

$$\chi(T) = \chi_0 + \frac{C}{T-\theta} \tag{3}$$

where $\chi_0$ represents the sum of all temperature independent contributions to the magnetic susceptibility, and $C$ and $\theta$ are the Curie constant and the Curie–Weiss temperature respectively. The results of the curve fits are listed in Table 1. Not all of the susceptibilities could be described by Eq. (3) in the whole temperature range; in those cases low temperature fits were used. The determined values of $C$ and $\theta$ allow us to estimate the susceptibility contributions of permanent magnetic moments at room temperature $\chi^{CW}(300\,K) = C/(300\,K-\theta)$. As can be seen in Table 1, prominent susceptibility contributions $\chi^{CW}(300\,K)$ are found in the samples with $x = 0.10$, 0.20 and 0.30 only. Since the whole solid solution series in this study was prepared from the same chemicals, we can exclude the possibility that the Curie–Weiss contributions in the latter three samples are caused by paramagnetic impurities. It is rather expected that, due to lattice imperfections or a slight non-stoichiometry, some of the chromium or vanadium atoms are present in the form of paramagnetic ions instead of being in a covalent bound state without a permanent magnetic moment.

## 4. Discussion

The linear temperature dependence of the thermopower suggests we analyse the properties of $Cr_{1-x}V_xSi_2$ solid solutions in terms of a free-electron model. According to this model [15], the thermopower of a metal in the phonon scattering region (i.e. well above the residual resistivity region) is given by

$$S = \pm\frac{\pi^2 k_B}{e}\frac{T}{T_F} \tag{4}$$

Here, the sign of the thermopower corresponds to the sign of the charge carriers, and $T_F$ is the Fermi temperature of the system which is determined by the carrier concentration $n$ according to $T_F = 4.231\times10^{-11}(n/\text{cm}^{-3})^{2/3}$ K.

With one less valence electron than chromium, each vanadium atom is expected to introduce one hole when substituted for chromium in $Cr_{1-x}V_xSi_2$. Since there are three formula units of $Cr_{1-x}V_xSi_2$ per unit cell volume $v$, the carrier concentration of the solid solutions can be calculated by $n = 3x/v$. Equivalently, we can use the molar volumes (Eq. (2)) of the solid solutions and express the carrier concentration as

$$n = \frac{N_A x}{V_{mol}} \tag{5}$$

The molar volumes of the $Cr_{1-x}V_xSi_2$ solid solutions are listed in Table 2. From these data, carrier concentrations and room temperature thermopowers were calculated using Eq. (5) and Eq. (4) respectively. The results are also given in Table 2. A calculated curve of room temperature thermopowers is shown in Fig. 5, together with the experimental data. Considering the fact that the free-electron model is hardly ever a good assumption with respect to the thermopower of metals (including most of the alkali and all of the monovalent noble metals) [15,16], the agreement between calculated and experimental values in Fig. 5 has to be considered remarkably good.

Eq. (5) does not allow us to calculate the carrier concentration of stoichiometric $CrSi_2$. But since the free-electron formula of Eq. (4) has been proven applicable in the rest of the solid solution series, this relation has been used in order to calculate the carrier concentration of $CrSi_2$ from its room temperature thermopower. The obtained carrier concentration, $7.4\times10^{20}$ cm$^{-3}$, corresponds to 0.027 charge carriers per formula unit. This is by far too high to be explained by a loss of material during the synthesis. A carrier concentration of this order of magnitude, however, seems to be rather typical of stoichiometric $CrSi_2$: hole concentrations of $6.3\times10^{20}$, $7.7\times10^{20}$

Table 2
Molar volumes $V_{mol}$ of $Cr_{1-x}V_xSi_2$ solid solutions. Values of the carrier concentration $n$, room temperature thermopower $S(300\,K)$, mobility $\mu$, and free-electron Pauli susceptibility $\chi^{Pauli,\,free}$ are calculated

| $x$ | $V_{mol}$ ($cm^3\,mol^{-1}$) | $n$ ($10^{22}\,cm^{-3}$) | $S(300\,K)$ ($\mu V\,K^{-1}$) | $\mu$ ($cm^2\,V^{-1}\,s^{-1}$) | $\chi^{Pauli,\,free}$ ($10^{-6}\,cm^3\,mol^{-1}$) |
|---|---|---|---|---|---|
| 0.00 | 21.71 | 0.074[a] | 73.5 | 1.57 | 4.34 |
| 0.10 | 21.87 | 0.267 | 31.3 | 0.91 | 6.70 |
| 0.20 | 22.04 | 0.538 | 19.6 | 1.25 | 8.53 |
| 0.30 | 22.16 | 0.815 | 14.9 | 1.23 | 9.85 |
| 0.39 | 22.22 | 1.065 | 12.5 | 1.01 | 10.80 |
| 0.49 | 22.34 | 1.329 | 10.7 | 1.08 | 11.68 |
| 0.74 | 22.98 | 1.929 | 8.4 | 1.62 | 13.61 |
| 1.00 | 23.16 | 2.600 | 6.9 | 3.79 | 15.15 |

[a] Calculated in order to match the experimental value of $S(300\,K)$.

and $3.9\times10^{20}$, for instance, have been reported by other groups [12–14]. The stoichiometric $CrSi_2$ sample has been enclosed in Fig. 5 with the carrier concentration deduced above.

Mobilities of the charge carriers have been calculated from the carrier concentrations and the room temperature resistivities of the solid solutions:

$$\mu = \frac{1}{ne\rho} \tag{6}$$

The results are listed in Table 2. An approximately composition independent room temperature mobility of $(1.1\pm0.2)\,cm^2\,V^{-1}\,s^{-1}$ is found for $x = 0.10$–$0.49$. Mobilities found in the vicinity of the end members are somewhat higher, but still of the same order of magnitude.

The magnetic susceptibility of the $Cr_{1-x}V_xSi_2$ solid solutions may be divided into three terms:

$$\chi(T) = \chi^{core} + \chi^{del} + \chi^{CW}(T) \tag{7}$$

where $\chi^{core}$ is the sum of the diamagnetic core susceptibilities, $\chi^{del}$ the contribution of delocalized charge carriers, and $\chi^{CW}(T)$ the Curie–Weiss-like paramagnetic contribution caused by permanent magnetic moments.

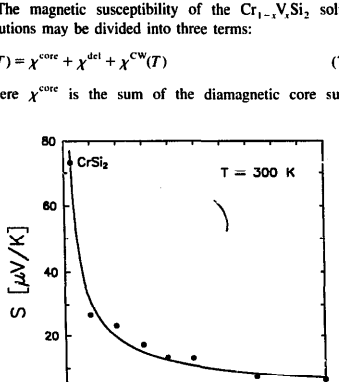


Fig. 5. Experimental (●) and calculated (———) room temperature thermopowers of $Cr_{1-x}V_xSi_2$ solid solutions.

The magnetic susceptibility of a degenerate electron gas is composed of a Pauli paramagnetic and a Landau diamagnetic term. If band structure effects are represented by an effective mass $m^*$, both contributions add up to

$$\chi^{del} = \chi^{Pauli,\,free}\left[\frac{m^*}{m_e} - \frac{1}{3}\frac{m_e}{m^*}\right] \tag{8}$$

where $\chi^{Pauli,\,free} = 2.208\times10^{-14}(n/cm^{-3})^{1/3}V_{mol}$ is the Pauli paramagnetic susceptibility of a degenerate free-electron gas and $m_e$ the free-electron mass [17].

The core diamagnetism of compounds is generally explained as the sum of diamagnetic ionic susceptibilities which can be taken from published tables. $CrSi_2$, however, is formed by strongly covalent chromium 3d–silicon 3p bonds [5], so an ionic picture is not appropriate in this case. But since vanadium is a neighbor of chromium in the periodic system of the elements and adopts an isoelectronic configuration with chromium when introducing a hole in $VSi_2$, the core susceptibilities of $CrSi_2$ and $VSi_2$ are expected to be rather similar. If we furthermore compare the calculated free-electron Pauli susceptibility of $VSi_2$ (Table 2) with the difference in the susceptibilities of $CrSi_2$ and $VSi_2$ at any temperature (Fig. 4), it becomes evident that an effective mass of at least $10\,m_e$ is to be expected in this compound. This large value of the effective mass allows us to neglect the diamagnetic term in Eq. (8), and Eq. (7) may therefore be rewritten as

$$\chi(T) - \chi^{CW}(T) = \chi^{core} + \frac{m^*}{m_e}\chi^{Pauli,\,free} \tag{9}$$

The magnetic susceptibilities of $Cr_{1-x}V_xSi_2$ solid solutions, corrected for Curie–Weiss contributions and plotted versus the calculated free-electron Pauli paramagnetisms, should therefore result in a straight line $y = a + bx$ with $a = \chi^{core}$ and $b = m^*/m_e$ at any temperature.

A plot of $\chi - \chi^{CW}$ vs. $\chi^{Pauli,\,free}$ at room temperature is shown in Fig. 6. Curie–Weiss contributions $\chi^{CW}(300\,K)$ and calculated free-electron Pauli susceptibilities $\chi^{Pauli,\,free}$

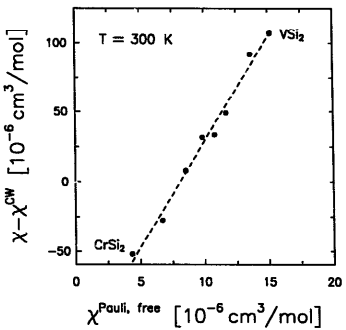


Fig. 6. Experimental room temperature susceptibilities of $Cr_{1-x}V_xSi_2$ solid solutions corrected for the contributions of permanent magnetic moments and plotted versus the calculated free-electron Pauli susceptibilities of Table 2. The dashed line represents a linear fit $y = a + bx$ with an intercept of $-123\times10^{-6}$ cm$^3$ mol$^{-1}$ and a slope of 15.2.

were taken from Tables 1 and 2 respectively. The good linearity of this plot confirms that the magnetic susceptibility of the solid solution series can be described by composition independent values of the core susceptibility and the effective mass. A linear best fit to the data gives $\chi^{core} = -123\times10^{-6}$ cm$^3$ mol$^{-1}$ and $m^* = 15.2\,m_e$. The latter values and Eq. (9) were used for the calculated curve of $\chi-\chi^{CW}$, which is shown in Fig. 7 together with experimental data. Calculated and observed data are in good agreement. This figure also shows that, because

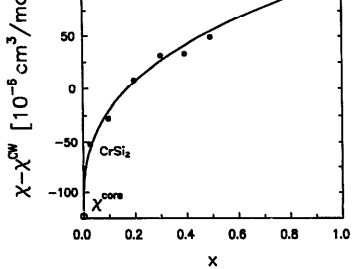


Fig. 7. Experimental (●) and calculated (———) room temperature susceptibilities of $Cr_{1-x}V_xSi_2$ solid solutions. The experimental room temperature susceptibilities have been corrected for contributions of permanent magnetic moments.

$\chi^{Pauli,\,free} \propto n^{1/3}$, even the low carrier concentration found in $CrSi_2$ causes a considerable susceptibility contribution. It would therefore be fallacious to simply ignore contributions of delocalized charge carriers in this compound.

The core diamagnetism of the $Cr_{1-x}V_xSi_2$ solid solutions found in this study is larger than the value reported for a $CrSi_2$ single crystal, $\chi^{core} = -83\times10^{-6}$ cm$^3$ mol$^{-1}$ [14]. This discrepancy is explained by the fact that a smaller effective mass was assumed for the holes in the latter study.

A composition independent and relatively large effective mass for the charge carriers in $Cr_{1-x}V_xSi_2$ solid solutions is in agreement with band structure calculations. Near $E_F$, energy band results are quite similar for $CrSi_2$ and $VSi_2$, and significant 3d orbital characters of the electronic states are found in both compounds [5]. The large value of the effective mass, however, makes it difficult to understand why the thermopower of the solid solutions is so well described using a free-electron model. An effective mass of $3.2\,m_e$ was derived in a previous study [13] for the holes in $CrSi_2$ from thermoelectric and Hall measurements; although this result is larger than the free-electron value, it is still much smaller than the value obtained from Fig. 6.

From Eq. (4) and Eq. (8), one can see that $S \propto m_S^{*} n^{-2/3}$ and $\chi^{Pauli,\,free} \propto m_\chi^{*} n^{1/3}$, where $m_S^*$ and $m_\chi^*$ represent effective masses affecting the thermopower and the magnetic susceptibilities. In order to resolve the discrepancy between the $m_S^*$ and $m_\chi^*$ values found in this study, one might assume that $z>1$ charge carriers are introduced per vanadium atom. However, consistent values for $m_S^*$ and $m_\chi^*$ without any change in Figs. 5 and 7 are obtained only for an unrealistic value of $z = 15.2$. It is also unlikely that the large paramagnetism of the charge carriers is exchange enhanced [18] rather than caused by a large effective mass: because the enhancement factor $(1+B_0)^{-1}$ of a Fermi liquid depends on the carrier concentration, it would not be possible to obtain linear behavior in Fig. 6.

Useful information which might help to clear up these points may be obtained by measurements of the specific heat at low temperature. We measured the specific heat of $Cr_{0.51}V_{0.49}Si_2$ between 2 and 15 K. The Sommerfeld parameter of the sample, $\gamma \approx 5\times10^{-3}$ J mol$^{-1}$ K$^{-2}$, is one order of magnitude larger than predicted by free-electron theory. This finding supports the idea of a large effective mass for the charge carriers in the $Cr_{1-x}V_xSi_2$ solid solution series.

## 5. Conclusions

Solid solutions of composition $Cr_{1-x}V_xSi_2$ have been prepared and investigated in the range $0\le x\le1$. Vegard's law is well obeyed for $x\le0.5$, whereas unit cell volumes for higher vanadium contents are larger than expected. Temperature dependent measurements of the thermopower,

the resistivity and the magnetic susceptibility of the samples reveal a continuous transition from degenerate semiconducting ($x = 0$) to metallic ($x = 1$) behavior. It is found that the thermoelectric figure of merit of $CrSi_2$ cannot be improved by alloying with $VSi_2$. The thermopower of the samples is well explained in terms of a free-electron model. A room temperature mobility of $\mu \approx 1.1\ cm^2\ V^{-1}\ s^{-1}$ is found for $0.1 \leq x \leq 0.5$. After correction for terms caused by permanent magnetic moments, the magnetic susceptibilities of the solid solutions can be accounted for by a core diamagnetism of $\chi^{core} = -123 \times 10^{-6}\ cm^3\ mol^{-1}$ and an effective mass of $m^* = 15\ m_e$.

## References


[1] M.C. Bost and J.E. Mahan, *J. Appl. Phys.*, *63* (1988) 839.

[2] B.K. Voronov, L.D. Dudkin and N.N. Trusova, *Sov. Phys. Crystallogr.*, *12* (1967) 448.

[3] T. Tokushima, I. Nishida, K. Sakata and T. Sakata, *J. Mater. Sci.*, *4* (1969) 978.

[4] M. Rowe (ed.), *CRC Handbook of Thermoelectrics*, CRC Press, New York, 1995.

[5] L.F. Mattheiss, *Phys. Rev. B*, *43* (1991) 12549.

[6] R.G. Long and J.E. Mahan, *Appl. Phys. Lett.*, *56* (1990) 1655.

[7] T.B. Massalski, *Binary Alloy Phase Diagrams*, American Society for Metals, Metals Park, OH, 1986.

[8] *JCPDS-ICDD*, PC-PDF Card Retrieval/Display System, Vers. 2.16, International Centre for Diffraction Data, PA, 1995.

[9] A.R. West, *Solid State Chemistry and its Applications*, Wiley, Chichester, 1989.

[10] W.B. Pearson, *Lattice Spacings and Structures of Metals and Alloys*, Pergamon Press, New York, 1958.

[11] T. Siegrist, personal communication, 1996.

[12] I. Nishida, *J. Mater. Sci.*, *7* (1972) 1119.

[13] I. Nishida and T. Sakata, *J. Phys. Chem. Solids*, *39* (1978) 499.

[14] I.J. Ohsugi, T. Kojima and I.A. Nishida, *Phys. Rev. B*, *42* (1990) 10761.

[15] F.J. Blatt, P.A. Schroeder, C.L. Foiles and D. Greig, *Thermoelectric Power of Metals*, Plenum Press, New York, 1976.

[16] A.H. Wilson, *The Theory of Metals*, Cambridge University Press, Cambridge, 2nd edn., 1958.

[17] G. Busch, A. Menth and B. Natterer, *Z. Naturforsch., 19a* (1964) 542.

[18] R.M. White, *Quantum Theory of Magnetism*, Springer, Berlin, 2nd edn., 1983.